remote sensing

MDPI

Article

Assessment of the Structural Integrity of the Roman Bridge of Alcántara (Spain) Using TLS and GPR

Juan Pedro Cortés Pérez, José Juan de Sanjosé Blasco, Alan D. J. Atkinson * and Luis Mariano del Río Pérez

Escuela Politécnica, Universidad de Extremadura, 10003 Cáceres, Spain; jpcortes@unex.es (J.P.C.P.); jjblasco@unex.es (J.J.d.S.B.); lmdelrio@unex.es (L.M.d.R.P.)

* Correspondence: atkinson@unex.es; Tel.: +34-927257578

Received: 16 December 2017; Accepted: 27 February 2018; Published: 2 March 2018

Abstract: The Roman bridge of Alcántara is the largest in Spain. Its preservation is of the utmost importance and to this end different aspects must be studied. The most prominent is the assessment of its structure, and this is especially important as the bridge remains in use. This paper documents the way the assessment of structural safety was carried out. The assessment methodology of existing structures was applied. The preliminary assessment was based on bibliographic data and non-destructive techniques. The geometric data of the bridge were obtained by Terrestrial Laser Scanning (TLS), which made possible the analysis of its deformations and assessment of its structure. Ground-Penetrating Radar (GPR) was also used with different antennae to work at different depths and spatial resolutions with the aim of analysing structural elements. From the above information, the assessment of structural safety was made using the limit analysis method by applying the historical works carried out on it and those described in the regulation of obligatory compliance in Spain (IAP11), studying the sensitivity of safety to the most relevant parameters. The state of preservation and structural integrity of the bridge is discussed and conclusions are drawn on the areas of greatest risk and the bases for the following assessment phase of preservation of the bridge.

Keywords: TLS; GPR; structural assessment; roman bridge; conservation

1. Introduction

The roman bridge of Alcántara and its surroundings, the Triumphal Arch and Temple, has been a Spanish National Monument since 13 August 1924, and is in the process of being declared a World Heritage Site by UNESCO. It was built across the river Tajo by Cayo Julio Lácer between 103 and 106 A.D. Its dimensions make it unique among Roman bridges. Its height from the river to the road over the bridge is 47 m and it boasts the largest arch span of the peninsular Roman bridges, with an arch of almost 29 m [1].

The bridge is 140 m long between buttresses and consists of six half-point arches on rectangular cross-section pillars with a triangular section cutwater upstream (Figure 1).

Owing to its heritage value, it has been analysed and studied through the ages by different authors. However, these studies have always centred on the historical aspect, its documentation as a cultural good and geometric study. However, this bridge, in addition to having great heritage value, is the infrastructure upon which the EX-207 Cáceres-Portugal road passes, with a mean daily intensity of 492 vehicles, 6% of these being heavy goods vehicles [2].

The bridge of Alcántara must also be analysed from a structural point of view in order to safeguard its preservation as a heritage site and the safety of its users. Thus, the aim of the research carried out was to provide information for the structural assessment of the bridge of Alcántara for its preservation, gathering information on its real geometry, any damage it has or has had, the materials that it is made of, the uses and interventions to which it is and has been subjected to, etc.

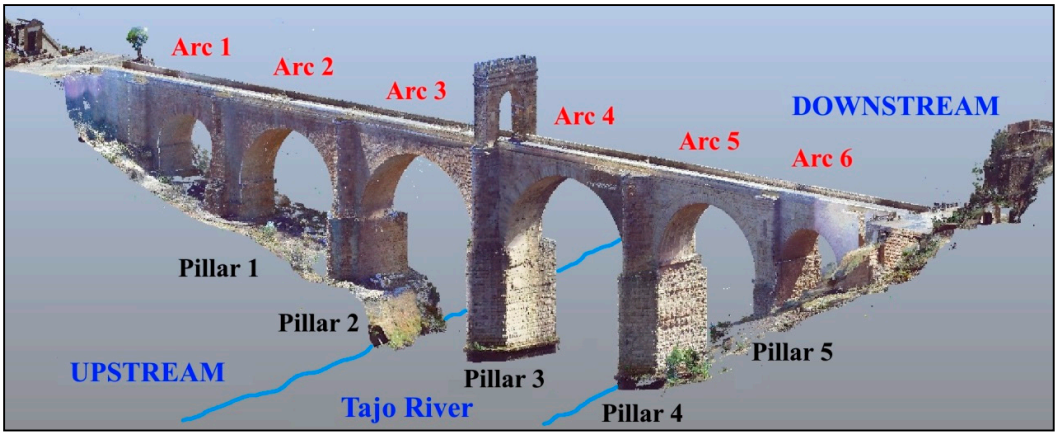

Figure 1. 3D view of the bridge of Alcántara using Terrestrial Laser Scanning (TLS) techniques.

2. Research Methodology

In accordance with the above considerations, the research methodology followed was based on the assessment methodology for existing structures included in the structure normatives [3,4] and previous research [5–8]. This methodology is based on assessment in phases, in which the depth of research must fit the type of assessment: preliminary or detailed (Figure 2). There must be a balance between the costs incurred in each phase, the data obtained and associated uncertainties. In this way, the most suitable research methods will be determined.

The management of the preservation of bridges requires the implantation of management systems [9], which a significant number of administrations, such as that of the Autonomous Community of Extremadura, do not have. Therefore, following the methodology described and with the aim that the research/assessment can be implemented in a future management system in such works in Extremadura, the research was centred on the preliminary assessment phase with an information update leading to a greater degree of precision in the assessment of safety. This will facilitate decision-making in matters of preservation as well as future detailed assessments.

As this is the first structural assessment of the bridge, research concentrated on the phases of anamnesis, analysis and diagnosis (Figure 2). The evaluation process ends when one of the phases produces an unequivocal conclusion that the structure is safe. In this research phase 1 is analyzed with the evaluation of the overall behavior of the bridge.

First of all, bibliographic research was conducted in order to collect information on the vicissitudes the bridge has undergone from the point of view of its preservation and any assessments or interventions made on it. In this phase, the information is updated relative to any interventions, its real geometry and the description of the materials that it is made of. It goes on to make a structural analysis from the data obtained in the previous phases before ending with a discussion of the results regarding safety by proposing what needs to be done in the short and medium term for the bridge's preservation.

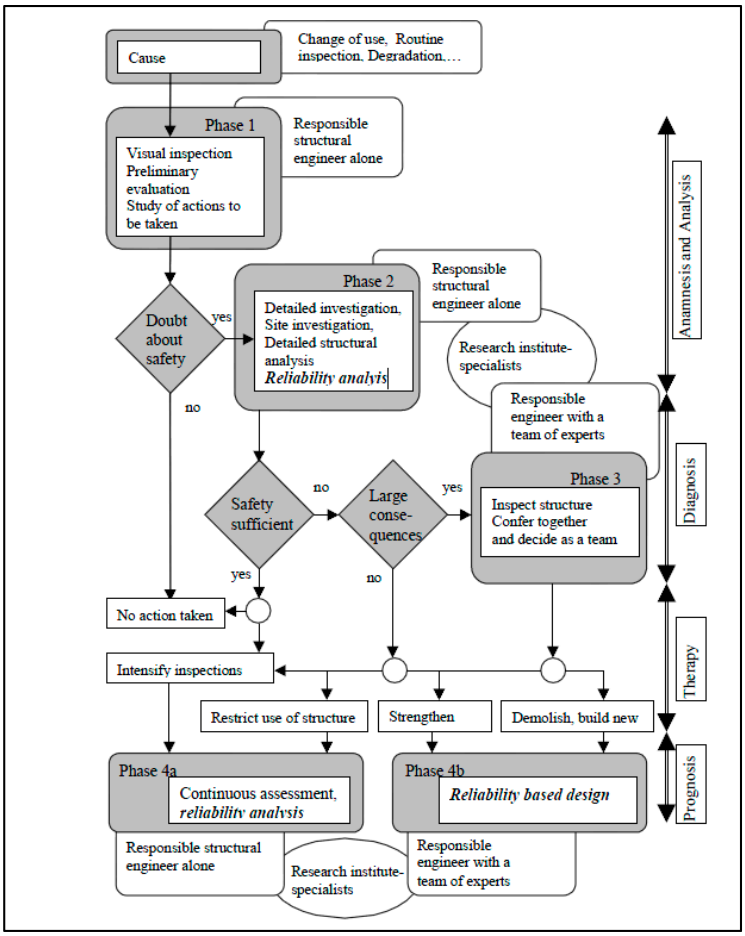

Figure 2. Flowchart of the assessment of historical structures [5].

3. Documentary Study for the Assessment of the Bridge of Alcántara

3.1. The Preservation of the Bridge through History

During its near twenty centuries of existence, the bridge of Alcántara has been subjected to human activity through wars and environmental events, mainly water-related, which have led to the destruction of part of its structure and have degraded it.

The most important damage was caused by wars, which mainly affected the arches. The first damage came in 1218 when King Alfonso XI ordered the destruction of the sixth arch [10]. The next time the destruction of arches was ordered was in the 15th century, but it was not finally carried out as Alfonso V, King of Portugal, withdrew in order to prevent the destruction [11]. In 1648 during the Restoration War between Portugal and Spain, the fifth arch was partially destroyed [12]. Finally, in 1809, as a result of the War of Independence, the fifth arch was completely destroyed [10,12]. To make the bridge functional once more, the missing arch was spanned by a hanging bridge until 1857, when the arch was rebuilt in a project of Alejandro Millán (Figure 3).

In addition to these complete or partial destructions of its arches, the bridge has suffered lesser damage [10,12,13] that has been repaired though there are no documentary details. In the reign of Carlos V (1543), the sixth arch, the fifth pillar, the right buttress and the central triumphal arch were restored. Later, between 1575 and 1577, Diego de Castañeda carried out some repairs to the stonework and elements in poor condition in pillar number 1 and the left buttress.

The document that describes the damage and its causes in greater detail is the report made in 1841 by the engineer Pelilla [14], in which he points out some damage owing to the filtration of

rainwater that "fall in channels between the joints in the ceilings of the arches" [14], producing the deterioration of the joints and even the loss of stones. The same situation is described by Alejandro Millán in 1857, who indicated that in one arch seven voussoirs had to be replaced as the granite disintegrated in their hands [15]. In this intervention, other repairs were also made [10,12], leaving the bridge in the state in which it now stands (Figure 3).

Figure 3. Photograph from downstream during the reconstruction work of the triumphal arch in 1857 after having reconstructed the fifth arch, which had been destroyed [16].

The other element that has done great damage is water flow, which has undermined the left part of pillar number 4 (Figure 4a), which had led to considerable cracking in its upper part, documented by the architect Diego de Ocha in 1804 [17], probably resulting from the river Tajo swelling up prior to 1763, this being the oldest date of the sheets recording water levels [18,19]. Attention was paid to the undermining of the pillar during the repair work of 1857, and was treated with rockfill at the base of the pillar to protect it [10]. However, the problem appeared once again in 1969 when the river ran dry during the construction work of a reservoir upstream. The pillar had lost the rockfill protection and a considerable number of stones, leaving a hollow 4 m high and 2 m deep along the 17 m of the side of the pillar [20] (Figure 4).

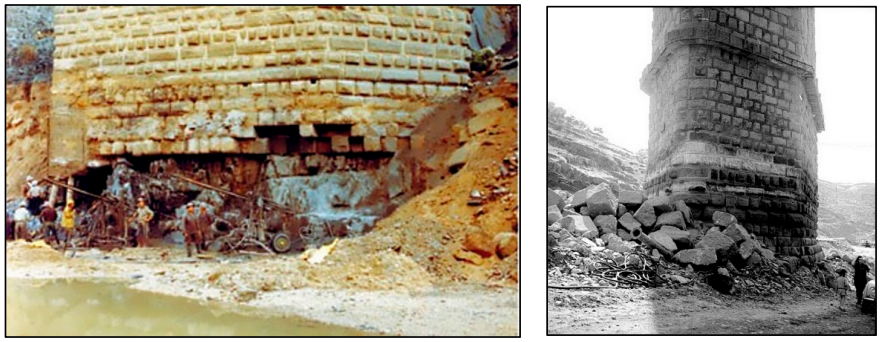

(**a**) (**b**)

Figure 4. (**a**) Repair work on the undermined pillar number 4 left side [20]. (**b**) Condition of pillar number 3 at the same time [21].

Finally, the bridge has been modified in such a way that its structural behaviour has been affected, and therefore its safety. The most important change was the elimination of the longitudinal slope of the bridge during the intervention by Millán in 1857. According to [18], over a length of 370 feet between the end of the bridge on the left and the triumphal arch, there was a rise of 10 feet and 5 inches in its height (Figure 5), meaning there would have been a slope of 2.7%. After taking it out, there was a fall

in the height by over 1.5 m (5 feet) in the surfaces over the larger arches, which reduced the capacity of load diffusion [22].

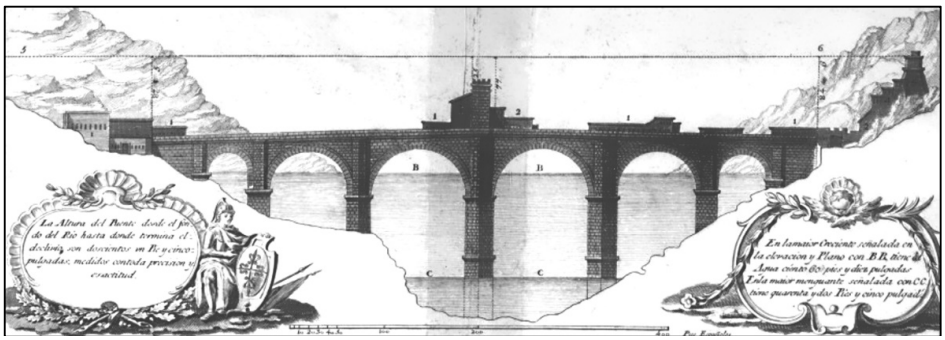

Figure 5. Print showing the variation in height between the ends of the bridge and the triumphal arch [23].

3.2. Update of the Interventions Made on the Bridge

Given the nature of the bridge, the most important interventions are weight-related: its own weight, dead loads and overloads due to road traffic as defined in the normative [24]. The assessment of interventions consisted of determining the characteristic values for the densities of dead loads, since according to the evolution of overloads on road bridges [25] the current values are higher than what the bridge could have been subjected to throughout its history.

In addition to considerations of weight, the bridge is subjected to hydrodynamic thrust [24] as defined by the following formula:

$$E = \left[\frac{1}{2}\rho V^2(T)\right] c_f A(T) \quad (1)$$

E—hydrodynamic thrust [N]; ρ—water density, equal to 1000 kg/m^3; $V(T)$—flowing velocity for flood flow of return period of T years [m/s]; c_f—coefficient of force (or drag) of the section that supports the thrust; $A(T)$—area of the element projected on a plane perpendicular to the flowing [m^2].

The parameters of the formula are defined in the normative, except *V(T)*: water velocity for flooding in the return period of T years. Throughout its history, the bridge has seen large floods, as reflected in the prints from historical documents [18,19,23]. More recently, we have reliable information of several floods in 1876, 1940, 1947, 1965 and 1970 (Figure 6), but in these later ones the water level remained below the level shown on the prints.

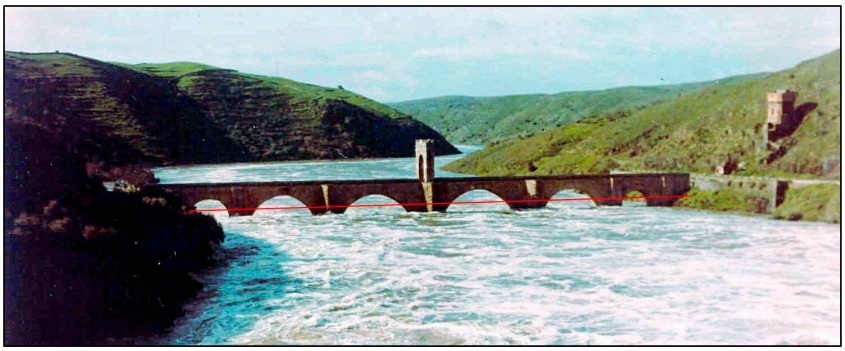

Figure 6. Flood of 1965. The flood level from the historical prints is marked by a red line [26].

The normative IAP11 indicates that seismic activity must be taken into account, but according to the normative [27] there is no need to consider it due to the bridge's location. Nevertheless, over its

long history, there is documented evidence that the bridge has been subjected to seismic activity, namely the Lisbon earthquake of 1755, which had an intensity of between 8.3 and 9 degrees on the Richter scale. In the town of Alcántara, it reached 5.5 degrees [28], causing damage to the Convent of San Benito (near the bridge), but no documents have been found mentioning any damage to the bridge.

3.3. Description of the Structure and Materials

Structurally, this is a bridge with stone arches supported on rectangular cross-section pillars with triangular cross-section cutwaters. At its ends, the arches are supported by buttresses, also of stone.

The transversal section of the bridge is similar to that of other Roman bridges [29], with the peculiarity that the material used in the filling of the arch vaults is stone [12,14,30], over which a granular filler [15] and granite paving stones are laid. These fillers are very important in the structural behaviour of this kind of bridges. The thickness of the filler is not known [22,31,32]. The tympana that serve to contain the fillers are also made of stone. According to [11,30] the arches are formed by two rings, a lower one of 1.6 m middle thickness and the upper one of 0.5 m.

The stonework was done without mortar [11,12,14] and was extracted from a quarry at a distance of one league (4.19 km) from the bridge [11,33]. In the research of this latter, the results of the petrographic analysis of the material were collected, and the material was determined as being entirely batolitic granite from Cáceres-Piedras Albas, which is also the source of the materials used to rebuild the arches [12].

4. Update of the Geometry, Fillers and Materials

To assess the structural aspect of the bridge fitted to the built reality, its geometry and the composition of fillers must be determined, as these are of fundamental importance to the behaviour of a factory bridge [22]. To do so, a survey of its geometry was conducted using Terrestrial Laser Scan (TLS) and an analysis of the fillers using ground penetrating radar (GPR).

4.1. Bridge Geometry Using TLS

To model the Roman bridge of Alcántara three-dimensionally, the terrestrial laser scanner (TLS) Faro Focus 3D X330 was used, which permits a massive collection of points (maximum velocity of measurement 976,000 points/s) in 3D with a precision of ±2 mm. From this data, the geometrical information of the bridge can be obtained and compared with the historical documentation, and the damage the bridge presents (cracks, deformations and slumps) [34–37].

The preparatory phase prior to emplacement included the decision on the recording technique to use. In the present project, scanning by the resection of targets was chosen given the large size of the bridge, and this resulted in the need for twelve emplacements to scan the whole bridge (Figure 7). The targets were placed such that each emplacement had a minimum of three targets. All the georeferenced scans of the bridge generated a cloud of 1200 million points, which were processed using the program "Trimble Realworks 6.5". Joining the different point clouds produced an error of less than 1 cm.

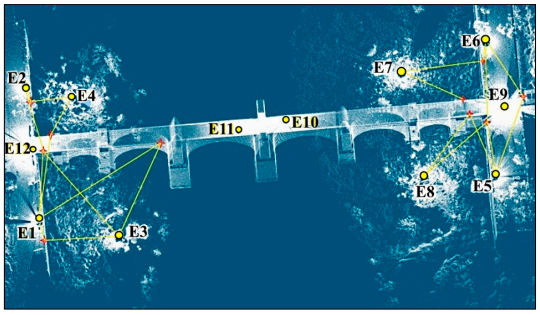

Figure 7. Location and joining-up of the 12 scans to measure the Roman bridge of Alcántara [38].

From georeferencing and joining up the point clouds, the next step was the elimination of residual points (noise), such as vegetation, urban objects, people and vehicles, unnecessary areas of ground, which gave the result of Figure 1. The number of points was thus reduced significantly, increasing processing capacity and speed. From the 3D modelling of the bridge, the longitudinal section (upstream and downstream) (Figure 8) and the transversal sections were obtained at each of the pillars (Figure 9).

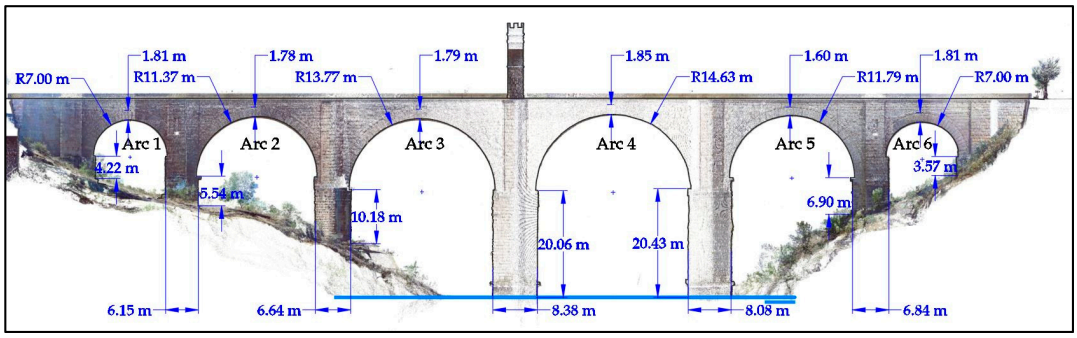

Figure 8. Longitudinal section downstream from the Roman bridge of Alcántara.

From the analysis of the geometry obtained by TLS, there were significant differences between the results obtained and the historical drawings and plans [1,10–12,14,15,20,33]. The dimensions of the bridge, as measured in different periods and by different authors, are shown in Table 1, in which the measurements are given in metres. Differences of up to 2.39 metres can be seen between the span of arch number 3, measured by Sánchez Taramás, and measurements made in the present study [38].

In the thickness of the arches, the lower ring has a thickness of 1.8 m. This does not happen in the reconstructed arch which has a thickness of 1.6 m. These measurements are greater than those indicated by [11] or [30].

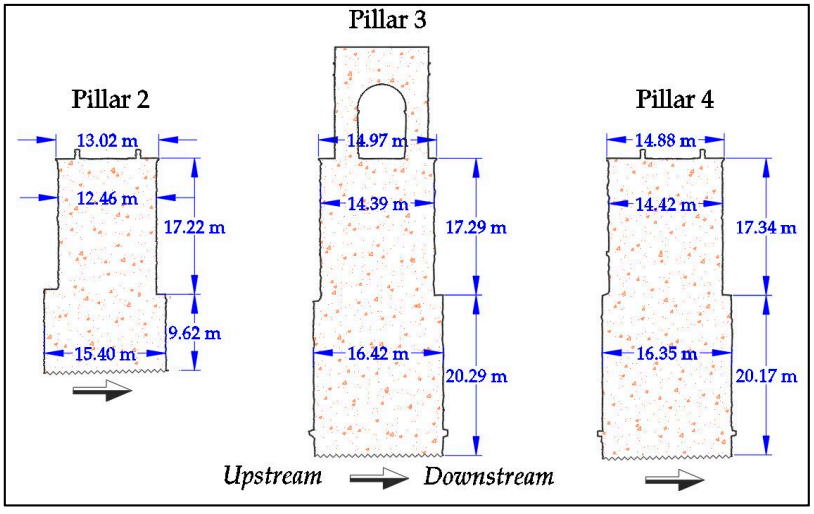

Figure 9. Transversal sections of pillars 2, 3 and 4.

In the case of the pillars, this difference in measurements through history is also seen. The central pillar, or pillar number 3, the most important in terms of its dimensions due to the role it plays in the formal composition of the bridge, was assigned a value by Fernando Rodríguez in 1797 [11,12,15,18,19] that was 2.30 m lower than the measurements taken for the present study by Angel Marras [38].

In the latest measurements taken in 2017, no collapse was detected in the bridge's pillars. The only variations observed on the vertical plane were those corresponding to recesses and protrusions of the

blocks as a result of drawing the characteristic dressed stone blocks of the bridge in representation of the standard sections (Figure 9).

Table 1. Dimensions (in metres) of the Roman bridge of Alcántara according to different authors.

Structural Element	Sanchez Taramás	Fernando Rodriguez	Fernandez Casado	Jesús Liz	Present Study
	1769	1797	1980	1988	2017
Arch no. 1	13.67	14.00		13.63	14.00
Arch no. 2	23.30	23.22		22.29	22.74
Arch no. 3	29.94	27.67	27.40	27.35	27.55
Arch no. 4	27.67	27.80	28.80	28.90	29.25
Arch no. 5	22.13	23.29	21.90		23.58
Arch no. 6	13.67	14.15	13.80		13.99
Pillar no. 1	-	5.57		5.98	6.17
Pillar no. 2		5.79		6.62	6.63
Pillar no. 3		6.00	8.30		8.30
Pillar no. 4		5.72			8.10
Pillar no. 5		5.57			6.84

4.2. Description of the Extrados Filling of the Bridge Using GPR

According to Section 3.3, the bridge is made up of an ashlar filling overlaid with another of granular material. The thickness of each, however, is not known or whether these fillers were altered during the various reconstructions the arches underwent. In order to obtain this information, the GPR technique was used, which is broadly applied in geology, geomorphology, architecture, civil engineering, forensic analysis and archaeology [39–44].

The equipment used for the fieldwork was the RAMAC of MÄLA Geoscience, with a central unit and two antennae of 200 and 500 MHz. In total, 217 spatial resolutions were provided by the antennae of approximately 16 cm and 7 cm ($\lambda/4$, $v \approx 0.13$ m/ns), respectively. We have considered time zero to the first air-ground reflection on the surface of the bridge.

A total of 12 radargrams were collected, seven of which were in the longitudinal direction (L1) of the bridge and five transversal (T1), with a total length of around 412 m (Table 2). With the aim of getting a first approximation of the scale of the depths in the radargrams, a reference velocity of v= 0.13 m/ns was used, which is compatible with the construction materials likely to have been used in the bridge: granite, sand, other rock fragments, etc. [45].

Table 2. Characteristics of the radargrams collected.

Radargram (Transect)	Antena (MHz)	Interval (m)	Observations
Prof 8 (L1)	200	0–85.9	Beginning of transect L1 with 200 MHz antenna in right buttress
Prof 9 (L1)	200	82.0–110.0	Partially overlapping Prof 8
Prof 10 (L1)	200	110–134.15	-
Prof 11 (L1)	200	134.15–173.3	
Prof 12 (L1)	200	173.3–190	End of transect L1 with 200 MHz antenna
Prof 16 (L1)	500	0–100.3	Depth parameters up to approx. 3 m
Prof 17 (L1)	500	0–92.9	Depth parameters up to approx. 1.5 m
Prof 13 (T1)	200	0–5.5	Adjacent to the triumphal arch. Left according to the water flow
Prof 14 (T1)	200	0–5.5	Centre of the opening of the triumphal arch. Right
Prof 15 (T1)	200	0–5.5	Pillar no. 5
Prof 18 (T1)	500	0–6.5	Idem Prof 13 right of the triumphal arch. Depth up to approx. 2 m
Prof 19 (T1)	500	0–6.5	Idem Prof 18. Depth up to approx. 4 m

Longitudinally, Figure 10 shows the composition of the elevation of the bridge and the composed radargram (Prof 8–Prof 12) of transect L1 with the 200 MHz antenna, which covers practically the entire length of the bridge in the W–E direction (≈190 m). Hyperbolic reflections are quite clearly observed, corresponding longitudinally with the location of the arches of the bridge. In depth, different layers more or less horizontal can be appreciated up to 20 ns (1 m, with v = 0.13 m/ns) approximately. Over these layers, the beginning of the different hyperbolic anomalies can be seen, which may correspond to the presence of granite stone making up the filler, as the arches of the bridge are at depths of over 3.5 m.

The hyperbolic anomaly detected in the central part at 40 ns is quite interesting because it does not correspond to any of the arches of the bridge. The anomaly is produced by the Triumphal Arch that is on the bridge. The radiograms Prof 8 to 12 were collected with a 200 MHz not shielded antenna. In some specific structures, these reflections can be seen with this antenna, as shown in Figure 10.

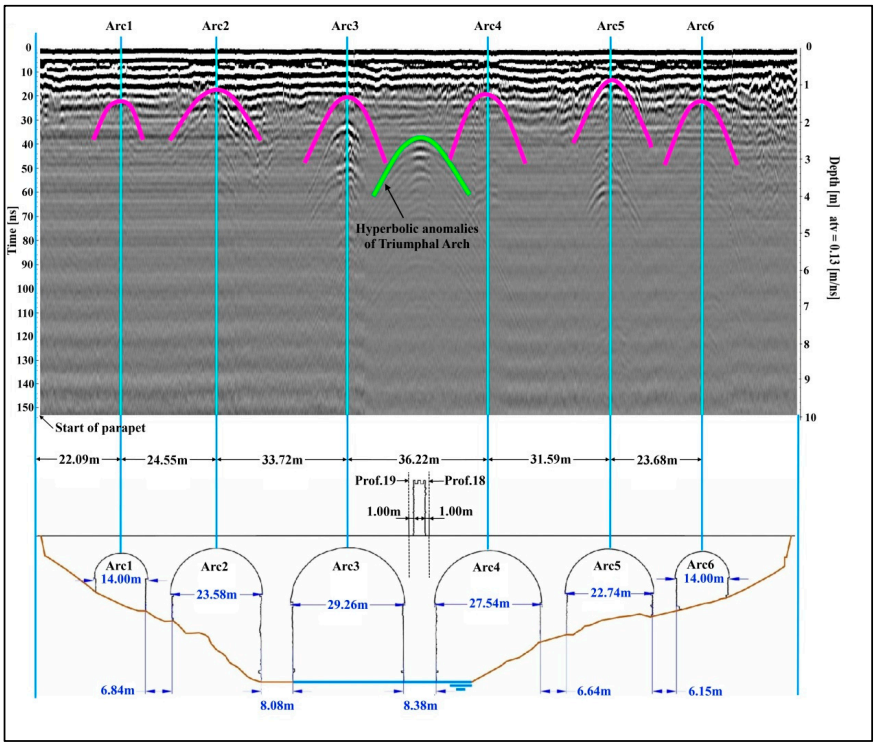

Figure 10. Radargrams Prof 8 to Prof 12 superimposed on the longitudinal elevation of the bridge from the TLS survey.

This is seen in more detail in radargrams Prof 16 and Prof 17 collected in the first 100 m with the 500 MHz antenna (Figures 11 and 12) and the equipment configured for maximum depths of 3.5 and 1.5 m respectively. In Prof 16, we can confirm the hypothesis of the anomaly produced by the Triumphal Arch, because when collecting the radargram with a shielded antenna, the anomaly does not appear after 90 m.

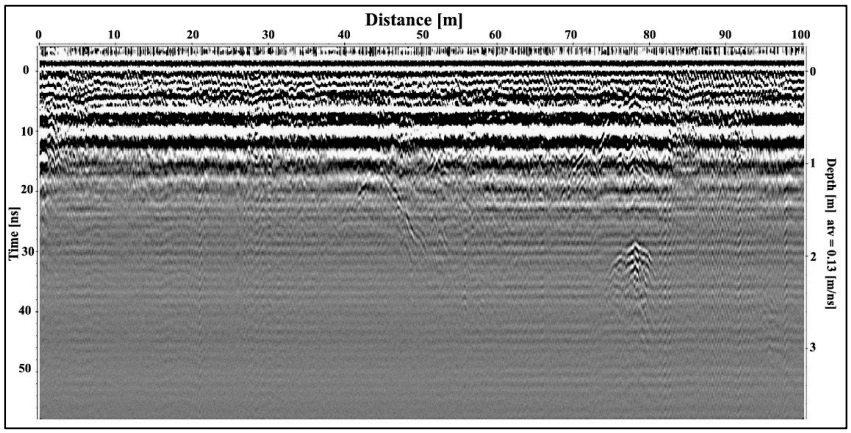

Figure 11. Radargram Prof 16 on transect L1, length 100.3 m and maximum depth 3.5 m, obtained by the 500 MHz antenna.

Figure 12 shows in greater detail the different strata of the bridge's filler. The first 20–25 cm would correspond to granite paving blocks, each of which is between approximately 5 and 10 cm thick. At greater depth, horizontal reflections are seen that configure an area up to a depth of 1 m made up of strata of greater thickness (around 20 cm) which may correspond to the different layers of the compacted ground filler.

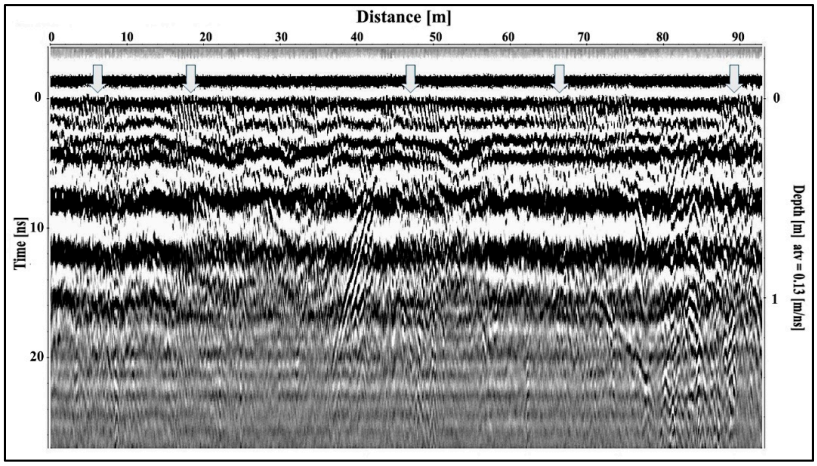

Figure 12. Radargram Prof 17 on the transect L1, length 92.9 m and maximum depth 1.5 m, obtained by the 500 MHz antenna.

Regarding the transversal plane, Figure 13 shows the radargrams Prof 18 and Prof 19 (500 MHz antenna). In both, the reflections can be clearly appreciated on the lateral walls of the bridge, as well as the different layers of paving and compacted ground. Radargram Prof 19 also reveals a clear horizontal reflection at around 30 ns of depth (≈2 m), which would correspond to the stonework. Nevertheless, in Figure 12, longitudinal, the hyperbolic anomalies appeared higher up in the keystones of arches 2, 3, 4 and 5.

One hypothesis to explain the reduction of the height of the anomaly between the longitudinal and the transversal data is that the filler is horizontal up to a depth of approximately 2 m. This strengthens the area of the kidneys of the arches, which is weaker in the arches. If the thickness of the arch is deducted in the middle of those arches, the resulting thicknesses are less than 2 m (Figure 8).

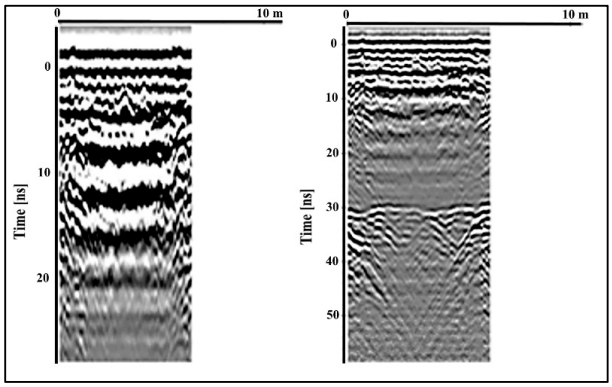

Figure 13. Radargrams Prof 18—left—and Prof 19—right—collected by the 500 MHz antenna on transect T1.

4.3. Update of the Description of the Ashlar Masonry

From what has been deduced from the study of the documents, the granite of the stonework is made up of coarse grain granite, often of the porphyritic type that forms part of the Iberian Massif [11],

the same geological formation investigated by Henriques et al., 2004 [46]. The resistant behaviour of this granite was researched in a considerable number of tests by Vasconcelos, 2005 [47], who proposed its characteristics of resistance (Table 3).

Table 3. Resistant characteristics of the granite of the bridge of Alcántara according to [47].

Density kg/m^3	Module of Deformation (MPa)	Compression Resistance (MPa)	Traction Resistance (MPa)	Poisson Coefficient
2645	11,028 (12.0) [1] to 59,993 (5.2) [1]	26.0 (7.1) [1] to 159.8 (2.5) [1]	1.56 (11.3) [1] to 8.08 (11.4) [1]	0.2 to 0.3

[1] The variation depends on the direction of the numbering according to the direction of effort. In brackets, the value of the coefficient of variation of the tests.

Vasconcelos (2005) [47] researched the resistance of the factory stonework as a whole by testing different types of stonework settling: without mortar, joints of different roughnesses and stonework on mortar of between 4.3 MPa and 5.8 MPa of compression resistance. From this study, he obtained as the compression resistance of the stonework in granite of medium resistance, a maximum resistance of 73.0 MPa in the case of stonework without mortar, and a minimum resistance of 18.4 MPa for the stonework with the mortar of least resistance. Regarding the modules of deformation, he obtained a maximum value of 14.72 MPa and a minimum of 1.25 MPa, respectively. The values of the angle of internal friction were practically unchanged at 0.65 (33°) and 0.63 (32°), respectively. Nevertheless, Mann Müller and Magenes, cited by Vasconcelos (2005) [47], give values of friction of 0.38 (21°) and 0.33 (18°), which may be associated with degraded masonry.

If Eurocode-6 [48] is applied with the values of Table 2, resistances of 7.18 MPa and 16.65 MPa are obtained. Ramos (2016) assigned a density of 22 kN/m^3 to the granular fillers of medium compactness, and an angle of internal friction of 30° [32].

5. Structural Analysis

5.1. Analysis of Factory Stonework Structures

The behaviour of factory structures is complex for different reasons: its low resistance to traction; lack of knowledge of the constructive process; difficulties in the precise description of the material when destructive tests are not possible, or because of the specific information they provide when tests can be carried out and the complexity of modelling.

Faced with these difficulties, there are researchers who propose analysis on three levels depending on the quantity and quality of the data required [49]. In the analysis on level I, the only data required are the geometrical and specific weight of the material using limit analysis and analysis of rigid blocks [22,50,51]. In addition to the aforementioned data, on level II the mechanical characteristics of the materials are needed and the analytical methods are elastic, checking for the non-linearity a posteriori, and geometric definition by means of bar elements. The analyses on level III require the definition of the constitutive law of the material and a more precise definition of the geometry and of the loading process in modelling the geometric and mechanical non-linearities of the factory stonework [52–54].

As may be observed, the grading of the level of analysis follows the assessment methodology by the phases presented in Figure 2. The assessment of the safety of the bridge of Alcántara was carried out on level I, as the materials were described using the documentary study. Further to overall safety and the most likely mechanisms of collapse, the influence of the variability of factory stonework in terms of its resistant behaviour was analysed.

5.2. Level I Analysis: Limit Analysis

The analysis was performed using the software Ring 2.0 [55], which has been applied in different research projects on factory bridges [56,57] (Figure 14). In this model, it was developed using the real defined geometry taking into consideration the way the fillers lay as deduced from the research using GRP and taking into account the vicissitudes that the structure has undergone.

The characteristics of the materials are presented in Section 3.3. From these data, a model of structural analysis was drawn up to study the safety of the bridge through the method of limit analysis for four geometric configurations:

- S0: original longitudinally sloping bridge. From the data of Bonet, 1991 [23].
- S1: demolition of arch no. 6, modelling arches 1 to 5 and longitudinal slope.
- S2: demolition of arch no. 5, modelling arches 1 to 4 and longitudinal slope.
- S3: entire bridge in the present condition.

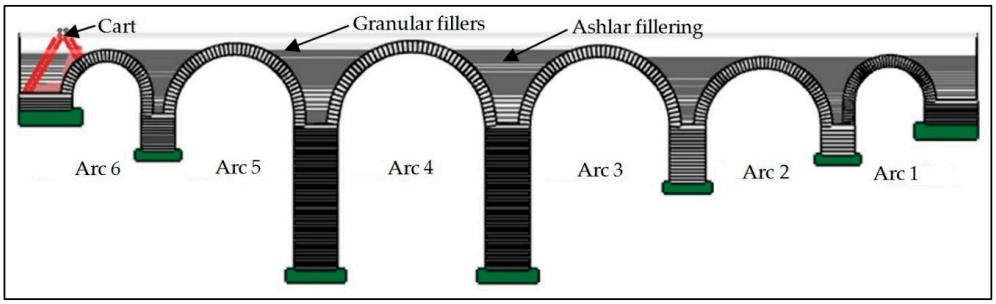

Figure 14. Model for analysis of level I.

Gravitational actions and vertical overloads were considered in the assessment. Seismic action was not considered since its application is not mandatory in the regulations [27] and the bridge does not present damage due to the Lisbon earthquake of 1755 [28].

In cases where there is no bridge action regulation, two loads of 60 kN separated by 3.0 m in positions S0 and S2 were considered. These corresponded to the loads exerted by a cart [25]. In positions S0 and S3, the load of the norm [24] of 600 kN was considered in order to compare the effect of the elimination of the slope according to the current normative and the degree of safety. Uniform loads were not considered due to the low intensity of traffic (492 vehicles/day) [2].

The static charge values indicated include the amplification of the dynamic effects by impact [24,58]. In the case of the Alcántara bridge, this amplification is practically non-existent because the speed limit is 30 km/h and there is no risk of resonance [59].

In these models, both strength at compression and slipping of stonework were considered, according to the current normative framework [24,48]. Similarly, the effect of the stonework on the diffusion of loads was taken into consideration, but not its passive force as it was not known whether the contact between the filler and the stonework arches was perfect. In the definition of the thickness of the vaults of the arches, a simple ring of ashlar masonry was considered, as it was not known whether there was a connection between the two, the characteristics of the friction between them nor whether the more interior ring of ashlar masonry is continuous.

Given that:

- Damage to the stonework dated at more than 500 years ago.
- There is no information as to the location of this damage, what has been repaired nor what damage there may still be.
- The fillers are very important to its structural behaviour [22,31,32].
- The degree of knowledge on the characteristics of the stonework of the bridge does not come from direct testing.
- The aim of this research is to survey its behaviour for more advanced stages of research.

A parametric analysis was made taking different resistant values of the factory stonework into consideration (Table 4).

Table 4. Types of rigid filler factory stonework and vaults of arches in the bridge of Alcántara.

	Material		
Resistant Parameter	**1**	**2**	**3**
Resistance to compression (MPa)	7.18	40	73
Angle of friction (°)	0.33 (18)	0.49 (26)	0.65 (33)

Concerning safety, density remains constant as degradation will only initially affect the outermost area. The combination of the parameters and model produced 15 combinations (Table 5).

Safety is defined by the method of Limit States. The failures analysed were collapse by mechanism and slipping. The load factors are those indicated in the normative. Regarding the load reduction factors of the materials, an initial value of 1.5 was established for resistance to compression of the factory stonework and for the friction between stones.

For each of the simulations carried out, the failure that gave the lowest load coefficient was obtained (the value by which the load must be multiplied to cause the collapse) (Table 5 result a), its value (Table 5 result b) and the position of the load that caused it (Table 5 result c). To evaluate the incidence of the variability of the resistances of the materials in the collapse of the bridge following the analysis using the initial parameters, the load reduction factor of the resistance to compression of the factory stonework was progressively increased until reaching collapse, leaving the coefficient of friction reduction fixed (Table 5 result d). Similarly, the coefficient of friction reduction was established (Table 5 result d).

Figure 15 shows an example of failure by slipping and by mechanism.

Table 5. Summary of the assessment of the bridge of Alcántara for different materials and for each circumstance the bridge has undergone.

Circumstance	Material											
	1				2				3			
	a [1]	b [2]	c [3]	d [4]	a [1]	b [2]	c [3]	d [4]	a [1]	b [2]	c [3]	d [4]
S0.1 (Cart)	D	29.0	A6	2.3/1.9	D	116.0	A6	>3.0/2.7	D	257.0	A6	>3.0/>3.0
S0.2 (IAP11)	D	4.8	A6	2.2/1.8	D	17.7	A6	>3.0/2.6	D	38.9	A6	>3.0/>3.0
S1	C	6.7	A5	2.2/1.7	C	61.8	A5	>3.0/2.4	C	114.0	A5	>3.0/>3.0
S2	Unstable				D	46.8	A4	>3.0/2.5	C	53.4	A4	>3.0/>3.0
S3	D	4.8	A6	2.5/1.8	D	17.7	A6	>3.0/2.6	D	38.5	A6	>3.0/>3.0

[1] D: slipping, C: mechanism of collapse. [2] Value of the load coefficient. [3] Number of the arch with the lowest load coefficient. [4] Load reduction factor of the strength to compression or friction, which causes the collapse.

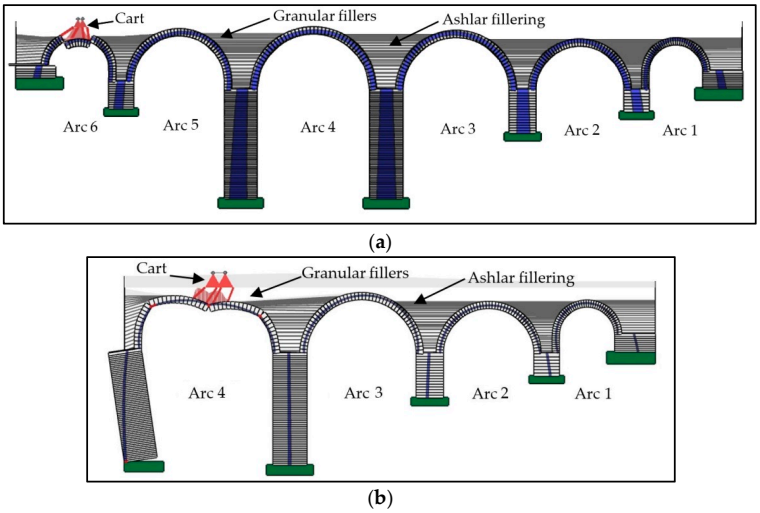

Figure 15. (**a**) Failure by slipping at position S0.1. (**b**) Failure by mechanism.

6. Discussion

Before this research was conducted, the differing geometric definitions of the bridge were highly varied with no way of knowing which was correct, which made a reliable structural assessment impossible. The geometric survey has provided the means by which to model the bridge with the required precision to make an assessment of it. Furthermore, the millimetrically precise definition of its geometry will allow detailed assessments to be drawn up. The application of TLS as a diagnostic technique [60] has made it possible to analyse the real deformation of the bridge, qualitatively checking that its behaviour is safe.

The GPR confirms that rigid stonework fillers are present in all of the pillars, not only in the broader arches, leading to more rigid behaviour, which would explain its stability in spite of the successive collapses of arches the bridge has undergone throughout its history.

The changing traffic crossing the bridge has reduced the safety of the bridge. If the load coefficient resulting from the three types of materials is compared between the situation of S0.1 and those of situation S3, safety is seen to have fallen by between 85% and 90%.

Nevertheless, the elimination of the longitudinal slope of the bridge has only produced a fall in safety of 1% in the worst-case scenario.

If we compare the load coefficients of the same situation as in Table 5, the degradation of the stonework, documented since over 500 years ago, gives rise to a considerable fall in safety. For example, if situation S3 is taken, the maximum fall would be 87% for a reduction in the resistance of the factory stonework of 90% and of 45% in friction.

An important general degradation of the factory stonework between 1809 and 1857 can be ruled out as the bridge would have collapsed had it been so, as shown by the result of S2 for the type I factory stonework (Table 5 material 1 result a).

Furthermore, it is evident that the failure mechanism determining the bridge's safety is the slipping of the stonework. Of the 15 simulations made, 67% of the failures were by slipping. To this it must be added that in all situations, on checking the influence of the uncertainty of the resistances, friction permits lower increases in the load reduction factor, which means greater sensitivity of the safety of the bridge to this strength parameter.

Of the conditions the bridge has been in, the one that led to the lowest safety levels was the demolition of arch number 5, which lasted from 1809 until 1857. Moreover, in the event of the exhaustion mechanism (Figure 15b) on the left side of the base of pillar number 4 in that condition, the stonework would open up. Taking into account that it is in this area that the loss of stonework took place before being repaired in 1857 and 1969 (Figure 4a), it can be confirmed that the origin of this loss was the opening of the joints in the stonework due to the imbalance of the thrust of arch number 4 following the demolition of arch number 5. This fissuring facilitated the entrance of water and the loss of the stones. Figure 4b shows the lower stones of pillar number 3 subjected to the same repairs. They only show signs of wear, since in that case the loads descend the pillar through the centre without causing tractions in its face (blue line in Figure 15b).

The documentary research revealed that the floods of the river Tajo in this area, which dated from the 19th century onwards, did not surpass the level described by M. Sánchez Taramás in the 17th century [23].

7. Conclusions

The structural safety of the bridge of Alcántara was assessed following the methodology described for historical structures. This assessment emphasised the importance of documentary research in structural analysis, as well as its development by phases.

As a result of this assessment being in its preliminary phase, the following conclusions are drawn with a view to carrying out more detailed research that will lead to a more precise assessment of the state of preservation and the degree of safety of the bridge.

1. It has been demonstrated how non-destructive techniques, such as TLS and GPR, are fundamental to perform the preliminary evaluation of masonry bridges reliably. The low cost of these techniques allows a reliable analysis of the safety of the structure. The real geometry is obtained through TLS and the GPR allows defining the configuration of the fillings. All these data are essential to evaluate the safety of a masonry bridge.
2. A considerable degradation in the stonework of the bridge has been confirmed, necessitating further general research into the state of preservation of stone and joints both in accessible and interior areas, since the interventions to date have only been carried out on accessible ones. The degradation of the stonework may lead to a local failure of the structure that cannot be detected using analytical models, neither local nor detailed.
3. Research must be made into the state of preservation of the areas of pillars 3 and 4, which are permanently underwater, in order to check the erosive effect of the water.
4. It needed a detailed study of the innermost ring of the arches to determine whether it can be taken into account from a structural point of view.
5. The reservoir upstream regulates floods. In order to manage the respectful rolling of floods with regard to the bridge, a study must be conducted to find the maximum hydrodynamic action the bridge can withstand without the collapse of or erosive damage to the stonework.
6. A detailed assessment should be made of the bridge's structural safety, a study to describe the factory stonework, paying particular attention to its resistance to slipping in the arches. This research must be carried out on a length in the area of the keystone of the arch, mainly in arch number 6. Moreover, it is important to study the variability of the results and their incidence on the load reduction factor. The description of the resistance to compression can be made with a lower level of study.

Acknowledgments: This research was made possible by funding granted by the Junta de Extremadura and the Fondo Europeo de Desarrollo Regional-FEDER, through the references GR15069 and GR15107 to the research groups NEXUS and COMPHAS respectively, to which the authors belong.

Author Contributions: Juan Pedro Cortés Pérez, conceived and designed the research. Juan Pedro Cortés Pérez has carried out the research and analysis of the results of the historical evolution, of the materials and of the structural evaluation. Juan Pedro Cortés Pérez wrote Sections 1–3, 4.3 and 5, Section 6 regarding the points investigated and Section 7. José Juan de Sanjosé Blasco and Alan D. J. Atkinson conceived and carried out the geometric survey with TLS, the comparative analysis of geometry, wrote Section 4.1 and the discussion of the results related to geometry. Luis Mariano del Río Pérez conceived, carried out and analyzed the research using GRP and wrote Section 4.2 and the discussion of GRP. Juan Pedro Cortés Pérez, José Juan de Sanjosé Blasco, Alan D. J. Atkinson and Luis Mariano del Río Pérez analyzed the final results and conceived the proposed new methodology.

Conflicts of Interest: The authors declare no conflict of interest.

References

1. Duran, M. Técnica y construcción de puentes romanos. In *Elementos de Ingeniería Romana*; Colegio de Ingenieros Técnicos de Obras Públicas: Salamanca, Spain, 2004; pp. 1–29.
2. De Extremadura, J. *Plan de Aforos de la Junta de Extremadura*; Junta de Extremadura: Mérida, Spain, 2010.
3. ISO13822. *Bases for Design of Structures—Assessment of Existing Structures*; ISO: Geneva, Switzerland, 2012.
4. DB-SE, C.T.E. *Codigo Técnico de la Edificación, Documento Básico: Seguridad Estructural*; BOE: Madrid, Spain, 2003; Volume 11.
5. Schueremans, L.; Van Rickstal, F.; Van Balen, K.; Van Gemert, Y.D. *Continuous Assessment of Historic Structures—A State of the Art osearch and Practice in Belgium*; ITAM-ARCCHIP: Louvain, Belgium, 2003; Volume 11, pp. 107–138.
6. Guedes Soares, C. *Safety and Reliability of Industrial Products, Systems and Structures*; CRC Press: Boca Raton, FL, USA, 2003; Volume 3, pp. 167–180.

7. Bucher, C.; Brehm, M.; Bolt, Y.H. Framework for assessment and life extension of existing structures and industrial plants. In *Safety and Reliability of Industrial Products, Systems and Structures*; CRC Press: Boca Raton, FL, USA, 2010; pp. 53–62.
8. Diamantidis, D.; Holický, Y.M. *Innovative Methods for the Assessment of Existing Structures*; Klokner Institute; Czech Technical University in Prague: Prague, Czech Republic, 2013.
9. De Fomento, M. *Guia Para la Realizacion de Inspecciones Principales de Obras de Paso en la Red de Carreteras del Estado*; Ministerio de Fomento: Madrid, Spain, 2012.
10. Pulgar, R.; del Carmen, M. *El Puente Romano de Alcántara: Reconstrucción en el Siglo XIX*; Institución Cultural El Brocense.: Cáceres, Spain, 1992.
11. Liz Guiral, J. *El Puente de Alcántara: Arqueología e Historia*; Fundación San Benito de Alcántara: Alcántara, Spain, 1988.
12. Cruz, M. El puente de Alcántara en los siglos XVII y XVIII: Noticias sobre su estado y planteamiento de restauración. *NORBA-ARTE* **2003**, *22–23*, 89–99.
13. Pizzo, A. El puente romano de Alcántara: Nueva documentación arqueológica y evidencias constructivas previas. *Arqueol. Arquit.* **2017**, *13*, 2–22. [CrossRef]
14. López García, M. Criterios de actuación en la reparación del puente de Alcántara: Respeto y economía. El informe del ingeniero Pelilla (1841). *OP Rev. Col. Ing. Caminos Canales Puertos* **2001**, *56*, 76–81.
15. De Obras Públicas, R. Millán, Obras de intervención en Puente de Alcántra por Alejandro. *Rev. Obras Públ.* **1857**, *1*, 12–13.
16. Fontanella, L. *Clifford en España (1849–1863): Un Fotógrafo en la Corte de Isabel II*; Ediciones El Viso: Madrid, Spain, 1999.
17. Crespo, D.; Grau, Y.M. Restaurar una obra pública en la época de la Ilustración: El puente de Alcántara. In *Congreso Nacional de Historia de la Construcción*; SEHC: Burgos, Spain, 2007; pp. 243–252.
18. Rodríguez, E. Plan y Elevación del Puente de Alcántara en la obra de Torres y Tapia. In *Crónica de la Orden de Caballería de Alcántara*; Librerías "París-Valencia": Madrid, Spain, 1763.
19. Taramás Sánchez, M. *Tratado de Fortificación, ó Arte de Construir los Edificios Militares, y Civiles de John Muller*; John Muller: Barcelona, Spain, 1769.
20. Fernández Troyano, L. Intervenciones en los puentes de piedra. *Ing. Territ. Restaur. Obra Públ.* **2011**, *92*, 42–49.
21. Moreno Gallo, I. Ingeniería Romana: PUENTES ROMANOS DE EXTREMADURA. Entre la Restauración y el Desastre. 2016. Available online: http://traianvsnet.blogspot.com.es/2016/09/puentes-romanos-entre-la-restauracion-y-el-desastre_21.html (accessed on 27 October 2017).
22. Martín-Caro, J.A. *Análisis Estructural de Puentes Arco de Fábrica: Criterios de Comprobación*; Universidad Politécnica de Madrid: Madrid, Spain, 2001.
23. Bonet Correa, A. *Cartografía Militar de Plazas Fuertes y Ciudades Españolas, Siglos XVII-XIX*; Instituto de Conservación y Restauración de Bienes Culturales: Madrid, Spain, 1991.
24. De Fomento, Y.M. *Instrucción Sobre las Acciones a Considerar en el Proyecto de Puentes de Carretera*; Madrid Ministerio de Fomento, Centro de Publicaciones: Madrid, Spain, 2011.
25. Cuvillo Mártinez-Ridruejo, Á. Trenes de carga de puentes de carretera. *Rev. Obras Públ.* **2002**, *3424*, 39–50.
26. Arévalo, E. El Salvamento del Puente de Alcántara, Las Carreteras de Extremadura, 2013. Available online: https://lascarreterasdeextremadura.blogspot.com.es/2013/03/el-salvamento-del-puente-de-alcantara.html (accessed on 27 October 2017).
27. De Fomento, Y.M. *Norma de Construcción Sismorresistente: Puentes*; Ministerio de Fomento, Dirección General del Instituto Geográfico Nacional: Madrid, Spain, 2007.
28. Mezcua, J.; Martínez Solares, Y.J.M. Sismicidad del Area Ibero-Magrebi. Instituto Geográfico Nacional, Madrid. 1983. Available online: https://www.researchgate.net/publication/40941361_Sismicidad_del_Area_Ibero-Magrebi (accessed on 2 March 2018).
29. Galliazzo, V. I PONTI ROMANI. In *II Congreso de las Obras Públicas Romanas*; CoITOP: Tarragona, Spain, 2004; pp. 9–23.
30. Fuentes, M.D. Estudio sobre las bóvedas de los puentes romanos. In *Nuevos Elementos de Ingeniería Romana*; III Congreso de las Obras Públicas Romanas: Astorga, Spain, 2006; pp. 131–142.
31. Espejo Niño, S.; León González, Y.J. Influencia determinante del relleno rígido en el comportamiento de los puentes de bóvedas de fábrica. In *IV Congreso Internacional de Estructuras*; ACHE: Valencia, Spain, 2008.

32. Ramos Casquero, A. *Caracterización Estructural de los Rellenos Situados en el Trasdós de Bóvedas de Edificios Históricos*; UPM: Madrid, Spain, 2016.
33. Blanco Freijeiro, A.; Angulo Iñiguez, Y.D. *El Puente de Alcántara en su Contexto Histórico: Discurso de Ingreso*; Real Academia de la Historia: Madrid, Spain, 1977.
34. Kaasalainen, S.; Jaakkola, A.; Kaasalainen, M.; Krooks, A.; Kukko, Y.A. Analysis of Incidence Angle and Distance Effects on Terrestrial Laser Scanner Intensity: Search for Correction Methods. *Remote Sens.* **2011**, *3*, 2207–2221. [CrossRef]
35. Vezočnik, R.; Ambrožič, T.; Sterle, O.; Bilban, G.; Pfeifer, N.; Stopar, Y.B. Use of Terrestrial Laser Scanning Technology for Long Term High Precision Deformation Monitoring. *Sensors* **2009**, *9*, 9873–9895. [CrossRef] [PubMed]
36. Cortés, J.P.; Berenguer, F.; Trancón, A.; de Sanjosé, Y.J.J. Análisis de daños del puente romano de Alcántara y la Catedral de Coria. In *Congreso X TOPCART*; CoITT: Madrid, Spain, 2012.
37. Xu, Z.; Wu, L.; Shen, Y.; Li, F.; Wang, Q.; Wang, Y.R. Tridimensional Reconstruction Applied to Cultural Heritage with the Use of Camera-Equipped UAV and Terrestrial Laser Scanner. *Remote Sens.* **2014**, *6*, 10413–10434. [CrossRef]
38. Marra, A. *Auscultación de Bienes Patrimoniales*; Universidad de Extremadura: Badajoz, Spain, 2017.
39. Goodman, D.; Piro, Y.S. GPR Imaging on Historical Buildings and Structures. In *GPR Remote Sensing in Archaeology*; Springer: Berlin/Heidelberg, Germany, 2013; pp. 143–157.
40. Del Rio, M.; Rico, I.; Serrano, E.; Tejado, Y.J.J. Applying GPR and Laser Scanner Techniques to Monitor the Ossoue Glacier (Pyrenees). *J. Environ. Eng. Geophys.* **2014**, *19*, 239–248. [CrossRef]
41. Czaja, K. Application of modeling of electromagnetic field and GPR measurements in investigations of antique tenement. EGU General Assembly Conference. 2012, 14, p. 8447. Available online: http://journals.bg.agh.edu.pl/GEOLOGY/2012.38.4/geol.2012.38.4.395.pdf (accessed on 2 March 2018).
42. Ranalli, D.; Scozzafava, M.; Tallini, Y.M. Ground penetrating radar investigations for the restoration of historic buildings: The case study of the Collemaggio Basilica (L'Aquila, Italy). *J. Cult. Herit.* **2004**, *5*, 91–99. [CrossRef]
43. Yelfm, R.J. Application of Ground Penetrating Radar to Civil and Geotechnical Engineering. *Electromag. Phenom.* **2007**, *7*, 103–117.
44. Conyers, L.B.; Goodman, Y.D. *Ground-Penetrating Radar: An Introduction for Archaeologists*; Altamira Press: Walnut Creek, CA, USA, 1997.
45. Daniels, D.J. *Surface-Penetrating Radar*; Institution of Electrical Engineers: Stevenage, United Kingdom, 1996.
46. Henriques, J.P.; Lourenço, P.B.; Binda, L.; Anzani, Y.A. Testing and Modelling of Multiple-Leaf Masonry Walls under Shear and Compression. In Proceedings of the IV International Seminar Structure Analysis of Historic Constructions, Padova, Italy, 10–13 November 2004.
47. Vasconcelos, G.F.M. *Experimental Investigations on the Mechanics of Stone Masonry: Characterization of Granites and Behavior of Ancient Masonry Shear Walls*; Universidade do Minho: Guimaraes, Portugal, 2005.
48. Eurocódigo-6. *Proyecto de Estructuras de Fabrica, Parte 1-1: Reglas Generales Para Edificios. Reglas Para Fábrica y Fábrica Armada*; AENOR: Madrid, Spain, 1996.
49. Martínez, J.L. *Determinación Teórica y Experimental de Diagramas de Interacción de Esfuerzos en Estructuras de Fábrica y Aplicación al Análisis de Construcciones Históricas*; Tesis doctoral del Departamento de Mecáncia de los Medios Contínuos y Teoría de Estructuras ETS ICCP Universidad Politécnica de Madrid: Madrid, Spain, 2003.
50. Heyman, J. *Teoría, Historia y Restauración de Estructuras de Fábrica*; Centro de Estudios y Experimentación de Obras Públicas: Madrid, Spain, 1999.
51. Morer, P.; de Arteaga, I.; Armesto, J.; Arias, Y.P. Comparative structural analyses of masonry bridges: An application to the Cernadela Bridge. *J. Cult. Herit.* **2011**, *12*, 300–309. [CrossRef]
52. Vermeltfoort, A.V. Analysis and experiments of masonry arches. In *Historical Constructions*; Technische Universiteit Eindhoven: Eindhoven, the Netherlands, 2011.
53. Lourenço, P.; Milani, Y.G. Modeling masonry with limit analysis finite elements: Review, applications and new directions. In *Eleventh International Conference on Civil, Structural and Environmental Engineering Computing*; Civil-Comp Press: Kippen, UK, 2007.
54. Rosas, J.G.; Villegas, L.M.; Lorenzo, Y.D. Los modelos numéricos frente al comportamiento de elementos de fábrica ensayadas en laboratorio. *Inf. Constr.* **2001**, *53*, 37–47.

55. LimitState: Analysis & Design Software for Engineers. Available online: http://www.limitstate.com/ (accessed on 20 November 2017).
56. Gilbert, M. Limit analysis applied to masonry arch bridges: State-of-the-art and recent developments. *Int. Conf. Arch. Bridg.* **2007**, *1972*, 13–28.
57. Audenaert, A.; Beke, Y.J. Applicability analysis of 2D-models for masonry arch bridge assessment: Ring, Archie-M and the elasto-plastic model. *WSEAS Trans. Appl. Theor. Mech.* **2010**, *5*, 221–230.
58. AENOR. *Spanish National Annex to Eurocode 1: Actions on Structures—Part 2: Traffic Loads on Bridges*; AENOR: Madrid, Spain, 2009.
59. Maestre, A. *Modos de Vibración del Puente Romano de Alcántara Mediante Maqueta*; Universidad de Extremadura: Badajoz, Spain, 2013.
60. SanJosé, J.J.; Cortés Pérez, J.P.; Berenguer Sempere, F.; Trancón Miguel, Y.A. El láser escáner terrestre como técnica de diagnóstico en estructuras históricas de fábrica. In *Patorreb 2012: 4º Congreso de Patología y Rehabilitación de Edificios*; Santiago de Compostela Colexio Oficial de Arquitectura de Galicia D.L.: Santiago de Compostela, Spain, 2012; p. 77.